Geochemical Characterization of Geological Standard Rock Samples from Rare Earth Element Distribution Patterns Measured by Inductively Coupled Plasma Atomic Emission Spectrometry

Kazuhiro TOYODA and Hiroki HARAGUCHI*
Department of Chemistry, Faculty of Science, The University of Tokyo,
7-3-1, Hongo, Bunkyo-ku, Tokyo 113
(Received September 22, 1986)

Rare earth elements (REEs) in twelve standard rock samples have been determined by inductively coupled plasma atomic emission spectrometry after separation of diverse metal ions with cation exchange resin. These rock samples are old six standard rocks (W-1, BCR-1, AGV-1, GSP-1, JB-1, JG-1) and new six standard rocks (JB-2, JB-3, JA-1, JR-1, JR-2, JGb-1) issued from the Geological Survey of Japan. These samples are various types of igneous rocks, which show various shapes of the REE distribution patterns. Geochemical characteristics of these standard rock samples will be discussed from the relationships between rock types and the shapes of the REE pattern.

In recent years, inductively coupled plasma atomic emission spectrometry (ICP-AES) has been extensively used as a convenient and sensitive analytical method for simultaneous multielement determination of geological samples.[1-6] The determination of various elements in the wide range of concentrations can be carried out by ICP-AES without matrix matching of the standard solutions.[1] The analytical sensitivities of REEs have been also improved by ICP-AES.[2-6] Thus, we have tried to perform simultaneous multielement determination of REEs in twelve geological standard rock samples issued from the Geological Survey of Japan.

The determination of rare earth elements have been receiving more attention in geological studies.[7] The behaviors of trace elements such as REEs during the process of genesis and differentiation of magma depend fundamentally on the distribution coefficients between melt and minerals.[8] On the basis of this assumption, for example, mutual genetic relationships of various rock types, such as tholeiitic and alkali rocks, has been studied. Petrogenetic studies of igneous rocks involve the determination of the history of the sources of melts, the conditions of melting, the chemical composition of the sources during melt, melting process and so forth. Since REEs are the most useful elements for such a geochemical study, precise analysis of REEs and trace element modeling using the element distribution coefficients (K_d) in mineral-melt systems have been examined.[7] Then it has been noted that REEs are significantly valuable for placing limits on the applicability of proposed petrogenetic models. Moreover, the REE patterns do not change so significantly through the process of alternation and metamorphism, because REEs belong to the group of chemically resembled elements and are strong to weathering.[9,10] Thus the behaviors of REEs during the melting and differentiation of igneous rock are explained mathematically by the Masuda-Coryell plot REE distribution pattern[11] which is the plot of the REE contents normalized to chondrite abundance.

Genetic classification and characterization of igneous rocks are commonly made by major chemical composition as well as mineral compositions.[13-15] Such classification and characterization, however, are sometimes done by the survey of minor element compositions, for example, first-row transition metal abundance patterns,[16,17] Sr/Ca-Ba/Ca systematics,[18] incompatible element patterns,[19,20] various ratios of two elements[8] and so on. Among the studies of trace elements for geological rock samples, the REE pattern is most popular and useful. Hence, in the present study, the determination of REEs in twelve geological standard rock samples has been performed by ICP-AES; JB-1 (alkali basalt), JB-2 (tholeiitic basalt), JB-3 (high aluminum basalt), BCR-1 (andesine tracky basalt), W-1 (dolelite), JGb-1 (gabbro), AGV-1 (trachy andesite), JA-1 (tholeiitic andesite), JR-1 and JR-2 (rhyolite), JG-1 and GSP-1 (granodiolite). The analytical results have been compared with the literature values,[22,23] which have been mainly determined by isotope dilution mass spectrometry (IDMS) and neutron activation analysis (NAA). Furthermore, the relationship between rock types and the shape of the REE patterns of twelve rock samples will be discussed according to knowledge of REE geochemistry.

Experimental

Instrument. An ICP emission spectrometer used is Jarrell-Ash model 975 Atom Comp MKII with some laboratory modification. The instrumental components and operating parameters for the emission measurements are summarized in Table 1. The analytical lines employed are shown in Table 2. The calibration curves were made by using low (blank) and high standard solutions.

Chemicals and Standard Solution. All the chemicals used were of analytical reagent grade. All the stock solutions (1000 $\mu g\ ml^{-1}$) were prepared from pure metals or oxides, and their concentrations were checked by the EDTA titration method with XO indicator. Working standard solutions for calibration curves were prepared by mixing the

Table 1. Operating Conditions for ICP-AES Measurement

RF power	1.1 kW
Gas flow rate	Coolant Ar gas 18 l min^{-1}
	Auxiliary Ar gas 1 l min^{-1}
	Carrier Ar gas 0.4 l min^{-1}
Observation height	16 mm above load coil
Nebulizer	Cross flow type
Spectrometer focal length	75 cm
Grating	2400 grooves mm^{-1}
Reciprocal linear dispersion	0.53 nm mm^{-1}
Slit width	Entrance slit 25 μm
	Exit slit 50 μm
Integration time	40 s
Internal standard	10 μg of Cd/ml
	[observed at 228.8 nm (2nd order)]

stock solutions into three groups, taking into consideration of minimizing mutual spectral interferences among rare earth elements. The combinations of elements for working standard solutions are summarized in Table 2. Standard IV contains internal standard element (Cd) and interferring elements (Y, Sc, Al, Fe, Zr, Cr), which could not be eliminated by chemical separation mentioned below. The internal standard was used to compensate possible fluctuations in nebulization or droplet transport. In order to minimize the variation of the nebulization efficiency due to the differences of the viscosities of the solutions, the acid content in each standard solution was adjusted to be 3 M (M=mol dm^{-3}) HCl so as to match those in the digested sample solutions.

Sample Digestion and Separation Procedure. Rock samples (0.5 g) were digested by two methods such as HF-HNO_3 acid digestion and Na_2CO_3 alkali fusion.[5] After digestion, the samples were dissolved to 50 ml with 1 M HCl. The solution was loaded onto a 20×1 cm column of 100-200 mesh AG50W-X8 cation exchange resin. The

Table 2. Compositions of Mixed Standard Solutions for Calibration Curves and Analytical Wavelengths

Standard I		Standard II		Standard III		Standard IV	
Concn	Wavelength	Concn	Wavelength	Concn	Wavelength	Concn	Wavelength
μg ml^{-1}	nm	μg ml^{-1}	nm	μg ml^{-1}	nm	μg ml^{-1}	nm
La 10	398.8	Nd 20	430.3	Pr 10	422.2	Cd 100	228.8
Ce 20	418.7	Sm 10	442.2	Eu 10	381.9	Sc 10	361.3
Gd 10	303.2	Tb 10	367.6	Dy 10	340.7	Y 10	377.4
Lu 10	261.5	Ho 10	345.6	Er 10	369.2	Al 100	308.2
		Yb 10	328.9	Tm 10	313.1	Fe 100	238.2
						Zr 10	349.6
						Cr 10	205.5

Table 3. Correction Coefficients for Spectral Interferences[a]

Element	La	Ce	Pr	Nd	Sm	Eu	Gd	Tb	Dy	Ho	Er	Tm	Yb	Lu
La	—	0.9	0.3	0.6	0.8	—	—	0.6	0.2	0.4	—	—	—	1.7
Ce	0.6	—	15.7	1.4	10.9	—	0.7	5.7	1.7	0.6	0.7	1.2	—	—
Pr	4.1	9.9	—	70.3	29.9	0.6	4.1	9.3	3.0	2.4	3.3	2.5	—	—
Nd	6.6	22.7	3.73	—	8.0	4.6	3.8	10.0	4.5	2.4	5.4	19.2	—	—
Sm	1.8	7.2	10.8	1.6	—	0.4	6.3	10.3	12.6	3.1	10.3	14.1	—	—
Eu	3.5	2.7	0.5	2.7	0.9	—	1.9	1.8	1.5	0.6	2.6	3.1	—	—
Gd	0.3	1.6	12.3	4.3	2.5	—	—	1.0	46.7	4.5	1.0	117.0	—	—
Tb	0.6	11.8	12.2	2.0	4.9	0.2	30.0	—	14.9	7.4	5.5	50.1	0.2	0.2
Dy	0.6	129.0	2.0	2.4	1.2	0.1	7.0	80.6	—	0.8	2.7	13.6	0.4	0.2
Ho	0.6	1.0	—	0.3	2.2	—	13.9	3.0	15.8	—	1.0	17.0	0.5	0.5
Er	—	16.0	—	8.9	0.9	—	5.3	34.0	11.0	1.3	—	15.1	—	—
Tm	—	0.9	0.4	—	0.8	—	36.1	0.8	4.7	6.5	0.8	—	0.4	0.2
Yb	6.5	0.8	—	—	—	—	5.7	1.0	0.5	1.6	15.0	44.1	—	0.6
Lu	0.3	0.5	1.8	—	—	—	—	—	0.9	—	—	0.8	—	—
Y	—	2.8	0.7	0.6	1.1	0.1	0.5	1.3	1.2	0.4	2.5	0.7	0.1	—
Sc	1.9	1.4	—	1.0	1.0	—	—	3.2	1.3	0.4	0.7	—	—	—
Al	—	0.7	0.5	—	—	—	—	—	—	—	—	—	0.7	—
Fe	—	0.7	—	—	—	—	—	1.8	1.7	—	—	—	—	42.7
Zr	—	80.0	0.4	0.4	—	—	1.6	1.1	12.2	2.3	0.6	17.8	—	—
Cr	—	0.5	0.4	0.2	1.4	—	13.9	1.4	8.3	—	—	4.6	—	—

a) The correction coefficient is expressed as the analyte concentration (ng ml^{-1}) equivalent to the background emission intensity which is provided with 1 μg ml^{-1} of major element.

column was first eluted with 130 ml of 2 M HNO_3 solution. The REEs on the resin were then eluted with 50 ml of 6 M HNO_3, and the eluent was taken in a Teflon beaker. The eluent was then evaporated to dryness on a hot plate. The residue was dissolved again with 5 ml of 3 M HCl, in which 10 μg ml^{-1} of Cd was added as an internal standard. These procedures were carried out for both acid-digested and alkali-fused samples in the same manner. The solutions were then used for the determination of REEs by ICP-AES. Major elements (Al, Fe, Ca, Mg, Na, and K) and interferring elements (Mn, Ti, V, Be, and Th) could be removed from the sample solutions through the above procedures. When removal of Fe was insufficient, Fe was further removed from eluted solution by solvent extraction with MIBK. Total yield of the whole procedure was 96—98%. Cadmium was chosen as the internal standard, because its emission profile in the plasma was similar to most REE profiles and it had no spectral interferences with the selected REE emission lines. It was also noticed that Cd originally contained in the samples were eliminated during the cation exchange separation.

Correction of Spectral Interferences. The influences of background emission intensities due to major elements were investigated by observing the intensity profiles near analytical lines of minor and trace elements. The profiles were obtained by moving the entrance slit horizontally. The profile measurements allowed to distinguish the emission signals caused by major elements (spectral interferences) or impurities. The spectral interference due to other REEs and interfering elements such as Zr, Sc, and Cr were estimated as the correction coefficient expressed as the analyte concentration (ng ml^{-1}) equivalent to the background emission intensity which was provided with 1 μg ml^{-1} of each major element. The correction coefficients of REEs and other diverse elements for spectral interference correction are summarized in Table 3.

Results

The detection limits in solution by ICP-AES are listed in Table 4, where the detection limits are defined as the analyte concentration corresponding to twice the standard deviation of background emission when the standard solution samples are nebulized into the ICP. The detection limits in rock sample are also listed in Table 4, along with the Leedey normarized values of REEs in Chondorite The detection limits in sample are evaluated from the detection limits in solution in case that 0.5 g of rock sample is digested and diluted to 5 ml. As can be seen in Table 4, the detection limits in sample are below the Leedey Chondrite abundance levels of REEs except Pr and Tb in geological samples. This means that the present experimental method is applicable to the determination of REEs in geological samples. After background correction, blank subtraction and spectral interference correction were carried out to obtain the analytical values for the standard rock samples. All the analytical values for REEs in JG-1, JB-1, AGV-1, BCR-1, W-1, and GSP-1 are summarized in Tables 5 and 6. Good agreement between the acid-digested and alkali-fused samples can be seen in terms of both AGV-1 and JB-1, and also the present data in five standard rocks except JG-1 are almost consistent with the literature values determined by NAA and IDMS. From these results it can be noted that the present method is suitable enough for the simultaneous multielement determination of all REEs except Tb and Tm. The analytical values for Tb and Tm were prone to serious interferences with the coexisting other REEs.

Recently it has been pointed out that the proposed values for heavy rare earth elements in JG-1 are not consistent, depending on the analytical methods. The values for heavy REEs in JG-1 obtained by NAA were about twice as much as the proposed values which were determined by IDMS technique.[23,25]

The present authors also pointed out in the previous paper[5] that the values of heavy REEs in JG-1 did not agree with each other, when the different decomposition methods were employed. As can be seen in Table 5, the values obtained by the alkali fusion preparation are about two times larger compared to those obtained by the acid digestion. The present values of REEs by acid digestion are almost identical with the values[23] formerly certified from GSJ, which were mainly determined by IDMS with acid digestion treatment. On the contrary, the REE values for the alkali fusion are consistent with those obtained by NAA.[25] These facts suggest that heavy REEs are enriched in some minerals which can not be completely decomposed by acid digestion. JG-1 is porphric biotite granodiorite, in which zircon is usually found as an accessory mineral. It is well known that zircon ($ZrSiO_4$) is not easily decomposed by acid digestion[26] and enriches heavy REEs.[7] In fact,

Table 4. Detection Limits (in Solution and in Sample) and Leedey Normalizing Values

Element	Detection limits		Leedey normalizing values
	in solution	in sample	
	ng ml^{-1}	μg g^{-1}	μg g^{-1}
La	4.4	0.044	0.378
Ce	21.2	0.212	0.976
Pr	18.7	0.187	0.136
Nd	15.0	0.150	0.716
Sm	12.4	0.124	0.230
Eu	0.8	0.008	0.0866
Gd	25.6	0.256	0.311
Tb	11.6	0.116	0.0589
Dy	14.2	0.142	0.390
Ho	3.4	0.034	0.0888
Er	3.6	0.036	0.255
Tm	11.0	0.110	0.0385
Yb	0.4	0.004	0.249
Lu	0.9	0.009	0.0387

from the determination of Zr in JG-1 decomposed by two different methods, it was found that Zr contents in JG-1 are 38 μg g^{-1} in acid digestion and 118 μg g^{-1} in alkali fusion, while the recommended value of Zr in JG-1 is 111 μg g^{-1}.[26] The difference of Zr values for JG-1 obtained by two decomposition methods may correspond to mean chemical composition of zircon which can not be dissolved by acid digestion. Then, GSP-1, JR-1, and JR-2, in which zircon is known to exist as an accessory mineral, were also decomposed by alkali-fusion method.

Discussion

The analytical values for 12 standard rock samples are summarized in Tables 5—7. As can be seen from these values, the concentrations of REEs in rock samples are characteristic, depending on the types of rock samples. Thus the geochemical features of standard rock samples will be discussed with emphasis on the REE patterns.

The REE patterns normalized by the Leedey normalizing factors are shown in Figs. 1—6, which were figured from the analytical data in Tables 5—7. Generally the REE patterns provide smooth curves

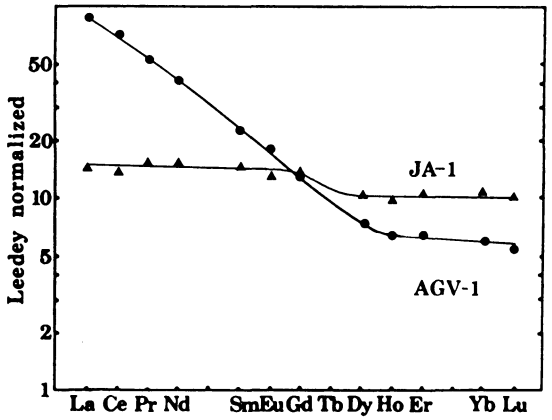

Fig. 3. REE patterns of JA-1 (tholeiitic andesite) and AGV-1 (trachy andesite).

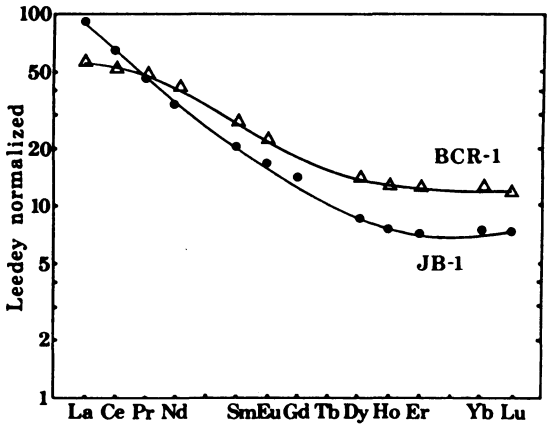

Fig. 1. REE patterns of BCR-1 (andesine tracky basalt) and JB-1 (alkali basalt)

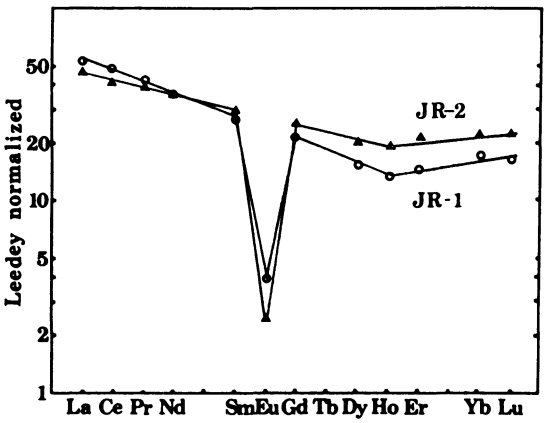

Fig. 4. REE patterns of JR-1 (rhyolite) and JR-2 (rhyolite).

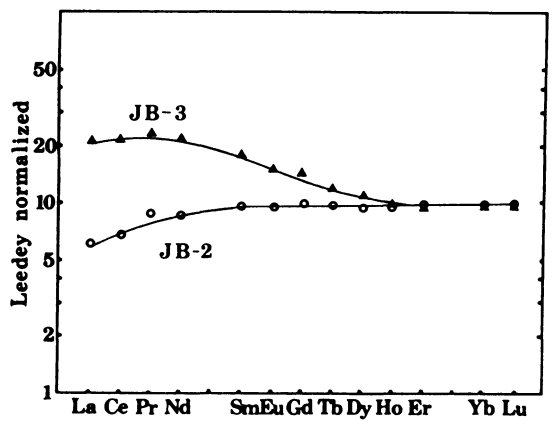

Fig. 2. REE patterns of JB-2 (tholeiitic basalt) and JB-3 (high aluminum basalt).

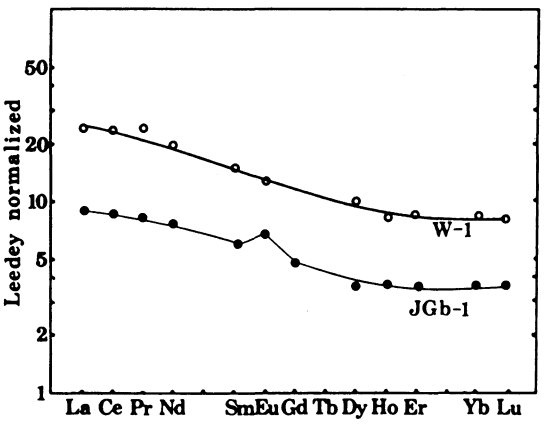

Fig. 5. REE patterns of W-1 (dolelite) and JGb-1 (gabbro).

except for Eu. Since Eu exists as the di- and tri-valent ions, it often shows some anomaly. Thus, these REE distribution patterns including Eu anomaly are useful to discuss some geochemical or geological characteristics of rock samples as well as their origin and classification.

Basalt. Masuda analyzed several basalts from Japan and found that basalts can be classified into three groups, based on general petrographic characteristics and REE patterns[27-29]; alkali basalt, tholeiitic basalt, and high aluminum basalt. Alkali basalt shows the REE pattern, in which light REEs are usually enriched, as is seen for JB-1 shown in Fig. 4. On the other hand, tholeiitic basalt contains less light REEs and show the rather flat pattern through all REE elements, which is seen in JB-2. The difference of these two REE patterns may be interpreted as follows. As has been known,[8] tholeiitic basalt magma and alkali olivine basalt magma have different genesis. The difference of the shapes of REE patterns mainly depends on degree of partial melting of upper mantle, when magma is generated from upper mantle. Already, this assumption has been elucidated by high pressure experiment in laboratory.[8,30,31] Most models for the formation of tholeiites assume about 20—30% melting of upper mantle peridotite with various REE contents, which reasonably explains the REE contents in tholeiites.[32] Tholeiites with low REE contents and flat REE distribution in Leedey-normalized curves are assumed to melt from primitive mantle with little or no

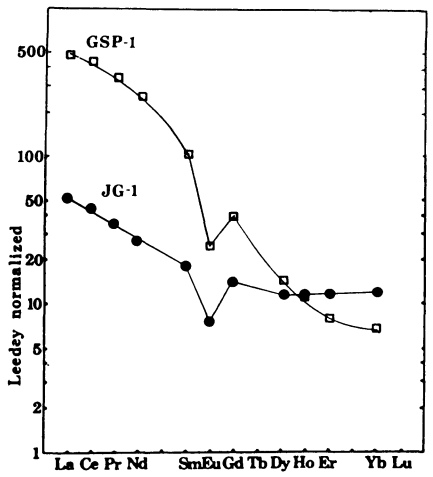

Fig. 6. REE patterns of JG-1 (granodiolite) and GSP-1 (granodiolite).

Table 6. Analytical Results of Standard Rock Samples[a]

	BCR-1		W-1		GSP-1	
	Found[b]	Ref. 22	Found[b]	Ref. 22	Found[c]	Ref. 22
La	22.1	25.0	10.3	10.9	182	183
Ce	50.5	53.7	23.0	23	428	406
Pr	6.7	6.9	3.3	3.2	54.5	51
Nd	29.1	28.7	14.5	15	186	190
Sm	6.4	6.58	3.5	3.5	26.1	26.8
Eu	1.8	1.96	1.1	1.11	2.3	2.36
Gd	—	6.68	—	3.9	12.8	13
Tb	—	1.05	—	0.65	—	1.36
Dy	5.4	6.35	4.2	3.9	5.5	5.4
Ho	1.1	1.25	0.73	0.81	—	1.2
Er	3.3	3.61	2.2	2.3	2.2	2.5
Tm	—	0.59	—	0.34	—	—
Yb	3.1	3.39	2.1	2.12	1.8	1.7
Lu	0.45	0.512	0.31	0.34	—	0.22

a) All values are in $\mu g\ g^{-1}$. b) Acid digestion. c) Alkali fusion.

Table 5. Analytical Results of Standard Rock Samples[a]

	JG-1			JB-1			AGV-1		
	Found[b]	Found[c]	Ref. 23	Found[b]	Found[c]	Ref. 23	Found[b]	Found[c]	Ref. 22
La	20.3	19.9	22	36.7	36.1	36	34.1	35.7	38
Ce	43.6	42.9	43	63.5	63.7	67	71.6	64.9	66
Pr	4.85	4.49	2.3	6.76	6.26	8.7	7.42	7.25	6.5
Nd	18.8	18.1	20.6	25.3	24.6	27	32.0	30.8	34
Sm	4.36	4.38	4.5	4.90	5.04	5.16	5.63	5.93	5.9
Eu	0.66	0.65	0.69	1.54	1.51	1.5	1.56	1.60	1.66
Gd	3.82	4.42	3.9	4.85	4.73	4.80	4.62	4.64	5.2
Tb	—	—	0.63	—	—	0.47	—	—	0.71
Dy	3.20	4.45	3.2	3.96	3.75	4.1	3.36	3.23	3.8
Ho	0.55	0.95	0.57	0.73	0.70	0.7	—	0.55	0.73
Er	1.68	2.96	1.60	2.19	2.15	2.23	1.91	1.67	1.61
Tm	—	—	—	—	—	—	—	—	0.32
Yb	1.63	3.03	1.5	2.00	2.10	2.1	1.96	1.68	1.67
Lu	—	—	0.23	—	—	0.3	—	—	0.28

a) All values are in $\mu g\ g^{-1}$. b) Acid digestion. c) Alkali fusion.

Table 7. Analytical Results of New Standard Rocks from GSJ[a)]

	JB-2[b)]	JB-3[b)]	JR-1[c)]	JR-2[c)]	JA-1[b)]	JGb-1[b)]
La	2.3±0.1	8.0±0.2	19.4±0.6	16.5±0.8	5.3±0.3	3.4±0.1
Ce	6.6±0.1	21.0±0.3	46.9±0.9	41.0±0.7	13.3±0.6	8.6±0.2
Pr	1.2±0.1	3.2±0.1	5.8±0.2	5.5±0.1	2.1±0.1	1.1±0.1
Nd	6.2±0.2	15.4±0.4	24.8±1.0	25.0±0.4	11.0±0.8	5.5±0.3
Sm	2.2±0.1	4.2±0.1	5.7±0.2	6.6±0.2	3.4±0.1	1.4±0.1
Eu	0.82±0.01	1.3±0.1	0.25±0.08	0.20±0.04	1.15±0.06	0.60±0.02
Gd	3.1±0.1	4.6±0.2	6.6±0.2	7.8±0.9	4.6±0.3	1.50±0.05
Tb	0.58±0.06	0.70±0.09	—	1.3±0.2	—	—
Dy	3.7±0.3	4.4±0.2	5.9±0.3	7.7±0.1	4.0±0.2	1.4±0.1
Ho	0.83±0.03	0.84±0.01	1.12±0.02	1.7±0.1	0.88±0.03	0.32±0.02
Er	2.5±0.1	2.5±0.1	3.7±0.1	5.2±0.1	2.7±0.2	0.91±0.02
Tm	—	—	—	—	—	—
Yb	2.5±0.1	2.5±0.1	4.2±0.2	5.3±0.1	2.7±0.1	0.90±0.02
Lu	0.38±0.01	0.37±0.01	0.62±0.06	0.84±0.05	0.40±0.05	0.14±0.02

a) All values are in $\mu g\ g^{-1}$. b) Acid digestion. c) Alkali fusion.

enrichment of the light REEs relative to the heavy REEs.[33)] On the other hand, the model for the formation of alkali basalt assumes about 0.8—2.9% partial melting and 4.5—5% garnet content in residue.[30)] Garnet, with its very large mineral/melt *D* value for heavy REEs,[31)] must also be present in the residue left after partial melting. BCR-1, which also belongs to alkali rock,[22)] have the REE pattern similar to JB-1, as shown in Fig. 1.

High aluminum basalt is aluminum-rich tholeiitic basalts whose composition of Al_2O_3 is over 17%. Generally high aluminum basalt shows chemical characteristics between alkali basalts and tholeiitic basalts.[34)] This can be seen from the slope of the REE pattern of JB-3 which is between those of JB-1 and JB-2, shown in Figs. 1 and 2.

Andesite and Ryolite. Andesitic magma is generally formed by fractional crystallization of plagioclase, amphibole, pyroxene, or magnetite from the more basic melts.[35,36)] Such crystallization models are common to explain tholeiitic trend. Tholeiitic andesites formed by crystallization have trend to show the flat pattern in Leedey-normalized curves. Its abundance of REEs is slightly increased, but the shapes of the REE patterns do not significantly change during forming andesitic magma from basaltic magma by crystallization differentiation. Then, AGV-1 (trachy andesite, in alkali series) shows the light REE-enriched pattern, while JA-1 (tholeiitic andesite) does rather flat REE pattern. This can be seen in the REE patterns shown Fig. 3.

JR-1 and JR-2 were collected from the same sampling location, and so their REE patterns and major chemical compositions should be similar to each other. This trend can be seen in their REE patterns shown in Fig. 4. In addition, negative Eu anomaly is remarkably observed for both JR-1 and JR-2, which are interpretated in terms of Eu^{2+} depletion in the melting process owing to the crystallization of Ca-feldsper. Since oxygen fugasity is very low in magma chamber, some part of Eu exists as Eu^{2+} which has similar ion radius with Ca^{2+}.[37,38)] The *D* values of REEs (except Eu) for plagioclase/melt are low, and then the concentration of REEs (except Eu) in melt slightly increases through crystallization process of plagioclase. In general, Eu is concentrated in plagioclase rather than other REEs when it precipitates from the magma. Thus the differentiated magma may develop larger negative Eu anomalies from original magma that may have little or no Eu anomaly.

Plutonic Rock. Dolerite (W-1) is hypoabyssal basaltic rock and gabbro (JGb-1) is plutonic basaltic rock. W-1 and JGb-1 generally have the properties between alkali and tholeiitic rocks, and they show small slope in the patterns with light REE-enriched abundance. Positive Eu anomaly is clearly seen in JGb-1, while it is not in W-1. It can be explained that magma of W-1 have been mixed with Eu positive substance such as anorthite.[10,39)]

In JG-1 and GSP-1, light REEs are significantly enriched with negative Eu anomaly. As is well noted,[40)] the origin and genesis of granite is very complicated.[41,42)] The range of granitic melts can be determined by melting a variety of sources (mantle basaltic magma, intermediate and felsic magma, sedimentary rocks etc.). Petrography and experimental petrology of granitic rock indicate a wide range of mineral parageneses due to differences in magma compositions, temperature, pressure, and contents of dissolved volatile species. In addition, granitic magma are very viscous, and so the assumption of complete separation of crystals and magma is not realistic. Then, it is still difficult to

propose an exact model using the REE pattern to help explain the petrogenesis of granitic melts. The REE patterns of JG-1 and GSP-1 cannot be well interpreted only by the present REE data.

Conclusion

The concentration of REEs in standard rock samples have been determined by ICP-AES. The REE patterns obtained from the present analytical data are useful to discuss the geological properties of standard rock samples along with the origins and genesis of these rock samples. From these experimental results and discussion it can be concluded that these standard rock samples can be used as the references in analysis as well as in geological or geochemical characterization of rock samples when their REE patterns can be obtained by proper analytical methods.

The present authors express sincere thanks to Hiroshi Shimizu and Kiyoshi Iwasaki for their valuable discussion. This research has been supported by the Grant-in-Aid for Scientific Research (No. 61030026) from the Ministry of Education, Science and Culture.

References

1) H. Tao, Y. Iwata, T. Hasegawa, Y. Nojiri, H. Haraguchi, and K. Fuwa, *Bull. Chem. Soc. Jpn.*, **56**, 1074 (1983).
2) J. G. Crock and F. E. Lichte, *Anal. Chem.*, **54**, 1329 (1982).
3) J. N. Walsh, F. Buckley, and J. Barker, *Chem. Geol.*, **33**, 141 (1981).
4) K. Yoshida and H. Haraguchi, *Anal. Chem.*, **56**, 2580 (1984).
5) K. Iwasaki, K. Fuwa, and H. Haraguchi, *Anal. Chim. Acta*, **183**, 239 (1986).
6) K. Toyoda and H. Haraguchi, *Chem. Lett.*, **1985**, 981.
7) G. N. Hanson, *Ann. Rev. Earth Planet. Sci. Lett.*, **8**, 381 (1980).
8) P. W. Gast, *Geochim. Cosmochim. Acta.*, **32**, 1057 (1968).
9) A. G. Herrmann and K. H. Wedepole, *Contri. Mineral. Petrol.*, **29**, 255 (1970).
10) T. H. Green, A. O. Brunfelt, and K. S. Heier, *Geochim. Cosmochim. Acta*, **36**, 241 (1972).
11) A. Masuda, *J. Earth Sci., Nagoya Univ.*, **10**, 173 (1962).
12) A. Masuda and Y. Matsui, *Geochim. Cosmochim. Acta*, **30**, 239 (1966).
13) E. A. K. Middlemost, *Bull. Volcanol.*, **36**, 382 (1972).
14) H. Kuno, *Bull. Volcanol.*, **219**, 195 (1966).
15) A. Miyashiro, *Am. J. Sci.*, **274**, 321 (1974)
16) J. A. Pearce and J. R. Cann, *Earth Planet. Sci. Lett.*, **19**, 290 (1973).
17) A. E. J. Engel, C. G. Engel, and R. G. Harvens, *Geol. Soc. Am. Bull.*, **76**, 719 (1965).
18) N. Onuma, M. Hirano, and N. Isshiki, *Geochem. J.*, **15**, 315 (1981).
19) J. A. Pearce and M. J. Norry, *Contrib. Mineral. Petrol.*, **69**, 33 (1979).
20) C. J. Hawkesworth, M. J. Norry, J. C. Roddick, and P. E. Baker, *Earth Planet. Sci. Lett.*, **42**, 45 (1979).
21) F. J. Flanagan, *Geochim. Cosmochim. Acta*, **31**, 289 (1967).
22) E. S. Gladney, C. E. Burns, and I. Roelandts, *Geostandards Newsletter*, **7**, 3 (1983).
23) A. Ando, *Bunseki*, **1984**, 597.
24) A. Ando, H. Kurasawa, T. Ohmori, and E. Takeda, *Geochem. J.*, **8**, 175 (1974).
25) M. Ebihara, Y. Minai, M. K. Kubo, T. Tominaga, N. Aota, T. Nikko, K. Sakamoto, and A. Ando, *Anal. Sci.*, **1**, 209 (1985).
26) H. Uchida, K. Iwasaki, and K. Tanaka, *Anal. Chim. Acta*, **134**, 375 (1982).
27) A. Masuda, *Geochem. J.*, **1**, 11 (1966).
28) A. Masuda, *Earth Planet. Sci. Lett.*, **4**, 284 (1968).
29) J. A. Philpotts, W. Martin, and C. C. Schnetzler, *Earth Planet. Sci. Lett.*, **12**, 89 (1971).
30) R. W. Kay and P. W. Gast, *J. Geol.*, **81**, 653 (1973).
31) S. S. Sun and G. N. Hanson, *Geology*, **3**, 297 (1975).
32) D. H. Green, *Earth Planet. Sci. Lett.*, **19**, 37 (1973).
33) Y. Masuda and K. Aoki, *Earth Planet. Sci. Lett.*, **39**, 289 (1978).
34) H. Kuno, *J. Petrogy*, **1**, 121 (1960).
35) S. R. Taylor, "Geochemistry of Andesites," in "Origin and Distribution of the Elements," ed by L. H. Ahrens, Pergamon Press, Oxford (1968), p. 559.
36) Y. Masuda and K. Aoki, *Earth Planet. Sci. Lett.*, **44**, 139 (1979).
37) J. A. Philpotts and C. C. Schnetzler, *Chem. Geol.*, **3**, 5 (1968).
38) J. A. Philpotts and C. C. Schnetzler, *Chem. Geol.* **4**, 464 (1969).
39) T. H. Green, A. O. Brunfelt, and K. S. Heier, *Earth Planet. Sci. Lett.*, **7**, 93 (1969).
40) G. N. Hanson, *Earth Planet. Sci. Lett.*, **38**, 26 (1978).
41) M. Takahashi, *Mem. Geol. Soc. Japan*, **25**, 225 (1985).
42) M. Takahashi, S. Aramaki, and S. Ishihara, *Mining Geol. Special Issue*, **8**, 13 (1980).